Microseismic monitoring of a reduced-scale dam: a case study with application of event characterization and ambient noise seismic interferometry

Igor Barbosa de Oliveira[*1,2], Pedro Canhaço de Assis[2,1], Fernando Sergio de Moraes[2,1], Igor Lopes Santana Braga[1,2], Sérgio Adriano Moura Oliveira[2,1], Geovane Frez Ouverney[1], Cleir Araujo Junior[1], Luciano Dias de Oliveira Pereira[1], Luiz Fernando Santana Braga[3,1], Rodolfo André Cardoso Neves[1] and Orlando Andrade de Moraes[1]
[1] Invision Geophysics, [2] LENEP/UENF, [3] SBGf

This paper was prepared for presentation during the 18th International Congress of the Brazilian Geophysical Society held in Rio de Janeiro, Brazil, 16-19 October 2023.

Abstract

Tailings dams are some of the largest man-made geotechnical structures. These containment facilities are susceptible to various failure processes, thus requiring systematic monitoring. A robust complementary alternative for assessing the safety of tailings dams, mining pits and other geotechnical structures is microseismic monitoring, which provides continuous information from the structure, not just on an on-off basis. This work describes field experiments on a reduced-scale dam built to test and improve the newly developed microseismic monitoring system. Field setup includes an instrument shed responsible for controlling the mesh network, storing and transmitting the collected microseismic data and filming the experiments. Several types of control routines keep track of the system's integrity and performance. These include evaluating the system's health, and stations' synchronism, testing the sensor arrays, and acquiring microseismic data for events characterization (active sources) and ambient noise seismic interferometry (passive sources). The results demonstrate the system capabilities and performance for characterizing induced microseismic events and estimating quantitative parameters such as event location in time and space and ground motion attributes following with the current state-of-the-art. Additionally the medium Green's function, computed using ambient noise seismic interferometry technique, was used to recover the coda wave velocity variation. Sixty days of continuous velocity variation monitoring of the reduced-scale reservoir structure shows a clear correlation of velocity variations with dry and wet periods verified by local pluviometry measurements and two filling-infiltration experiments conducted at the test site.

Introduction

According to Azam and Li (2010), tailings dams are some of the largest man-made geotechnical structures. And they are often built with steep slopes using the tailings themselves. As a result, these facilities are susceptible to various failure processes, thus requiring systematic monitoring.

Most dam monitoring techniques provide specific information about the structure's status, such as water level and pore pressure measurements. These tools are important in assessing safety; however, they often fail to indicate the first signs of failure.

A robust complementary alternative for assessing the safety of tailings dams, mining pits and other geotechnical structures is microseismic monitoring, which provides continuous information from the structure, not just on an on-off basis.

Microseismic monitoring is a geophysical technique with two modes of analysis. The more traditional approach is based on low-magnitude events caused by active sources from mining activity and other diverse causes. These events are identified, analyzed and processed to yield quantitative measurements that are of interest to the monitoring of tailings dams: such as ground motion measurements (PGD, PGV and PGA); events location in time and space; local and moment magnitudes.

The other approach employs seismic interferometry to process ambient noise data (passive monitoring), which allows for periodic reconstruction of a microseismic trace for each pair of microseismic station. This data can be used to estimate velocity variations within the structure or for more advanced methods of imaging and tomography.

In pursuing these microseismic applications, Invision Geophysics developed the Microseismic Monitoring System – M²S – to improve detection in monitored structures favoring timely intervention and maintenance to improve security levels (Braga *et al*., 2021). System development includes hardware and software from sensors and telemetry components designed to collect microseismic data continuously 24/7, to the backend for data storage and processing and the frontend for graphical visualization, reporting, issuing alerts, etc.

Figure 1 shows the main components of the microseismic sensors developed: (1) data acquisition and transmission module; (2) uniaxial geophone; (3) triaxial geophone; (4) spikes for coupling the geophones with the ground; (5) mesh network Wi-Fi antenna; (6) power supply; (7) signal cable for triaxial geophone; (8) signal cable for uniaxial geophone; (9) programming cable and (10) GPS antenna.

In this work we present a set of experiments that have been performed to test the newly developed microseismic monitoring system in a reduced-scale dam. The microseismic system operates in both passive and active source recording modes.

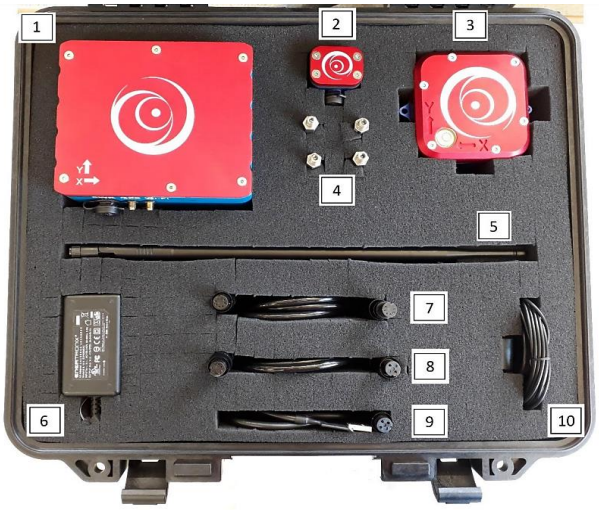

***Figure 1** – Main components of the microseismic sensors. Source: Braga et al., 2021*

Reduced-scale dam

A field test site with a reduced-scale dam was built to test the system. Microseismic monitoring requires a robust system to operate in harsh field conditions and high-precision sensors and components, granting proper synchronism between the stations and data quality. Another critical feature is system's control to monitor station health, and communication. Several tests involving different station layouts were conducted with microseismic data acquired for event characterization and for ambient noise seismic interferometry.

***Figure 2** – Reduced-scale dam instrumented with microseismic stations powered by solar energy*

***Figure 3** – Field instrument shed responsible for controlling the mesh network, storage and telemetry of microseismic data and filming of experiments*

***Figure 4** – The reduced-scale reservoir after the water filling-infiltration experiment*

Figure 2 shows the reduced-scale reservoir structure was built with clay rich landfill material over sand, having a storage capacity of approximately 10 m³. Notice the structure instrumentation composed by microseismic stations powered by solar energy.

An instrument shed (Figure 3) equipped for controlling the mesh network, storing and transmitting the microseismic data and for filming the experiments. Figure 4 shows a picture of filling-infiltration experiments performed at the site.

A mobile application monitors the system's health displaying in real-time various information about the microseismic stations in operation (Figure 5). The internal temperature of the stations and the monitoring center is an essential parameter to monitor to ensure proper operating conditions for the electronic components (Figure 6). Periodically, samples of the microseismic records collected by all stations are sent for initial quality control (Figure 7).

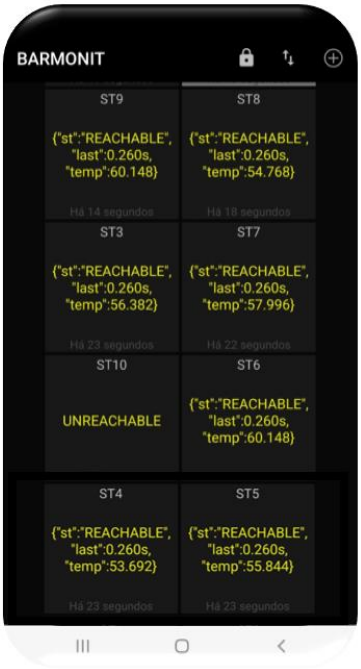

***Figure 5** – Mobile application providing real-time detailed system health information of individual microseismic stations*

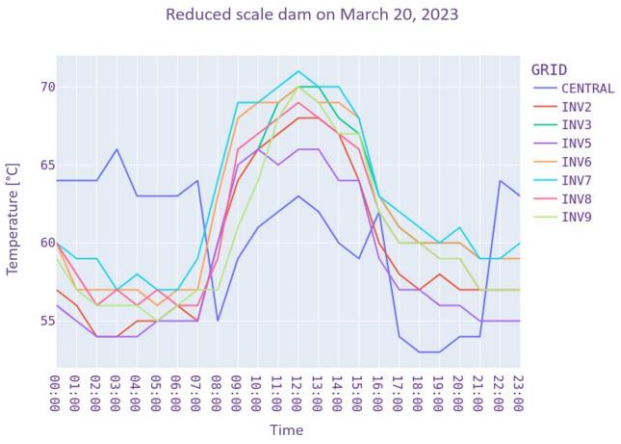

***Figure 6** – Internal temperature control of the stations and the equipment shed as part of the system health control App*

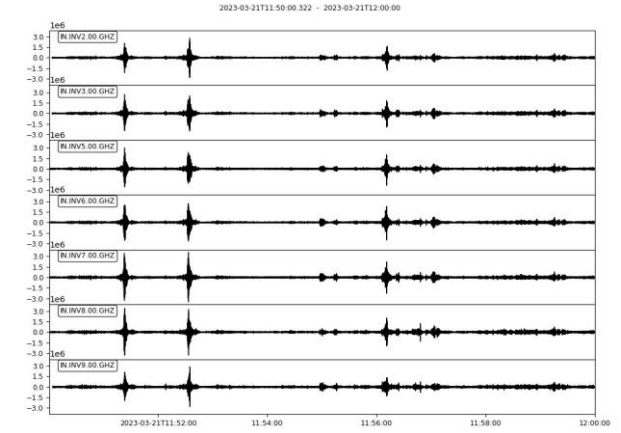

***Figure 7** – Example of a 10-minute microseismic data record, periodically collected by 7 stations and automatically sent by the application for quality control, processing, analysis and storage*

Figure 8 presents an example of a 24-hour plot for the microseismic records of station INV2. In this graph, there are 24 lines, each corresponding to a one-hour record, where we can observe the amplitude of vibrations over time. It is interesting to note the "silence" during the night and early morning, especially on the top traces. Also note the large number of events triggered during the day due to the activity of people, animals, vehicles and other sources of events.

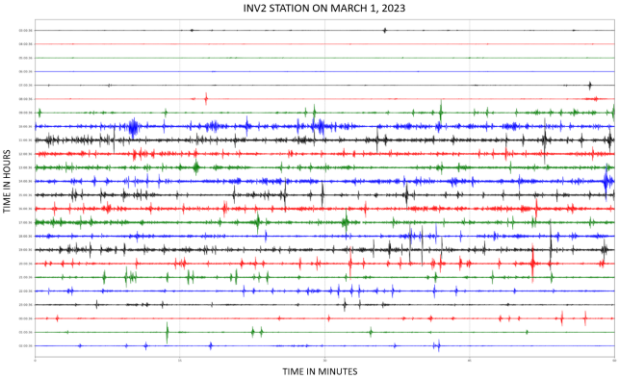

***Figure 8** – 24-hour microseismic data record for station INV2. The record is composed of 24 lines of one-our long trace record*

Microseismic event characterization

Figure 9 presents the processing workflow for triggered events detected by the sensors. Initially, these records are validated and stored in the database. Then each record on a different station is associated with a specific event and pre-processed to create an event record set for joint analysis. The analysis involves calculations of attributes such as peak ground velocity (PGV); peak ground acceleration (PGA) by trace differentiation; peak ground displacement (PGD) by trace integration; event location in time and space; hypocentral distance; local magnitude; corner frequency (signal's high-frequency limit); seismic potency; seismic moment and moment magnitude.

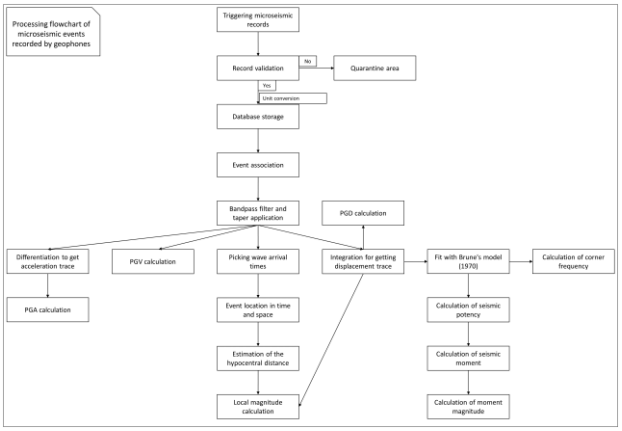

***Figure 9** – Microseismic event processing workflow*

Figure 10 shows the station layout map of 6 microseismic stations performed to test the event processing and analysis workflow. The red point indicates the position of the source consisting of a 10 kg sledgehammer.

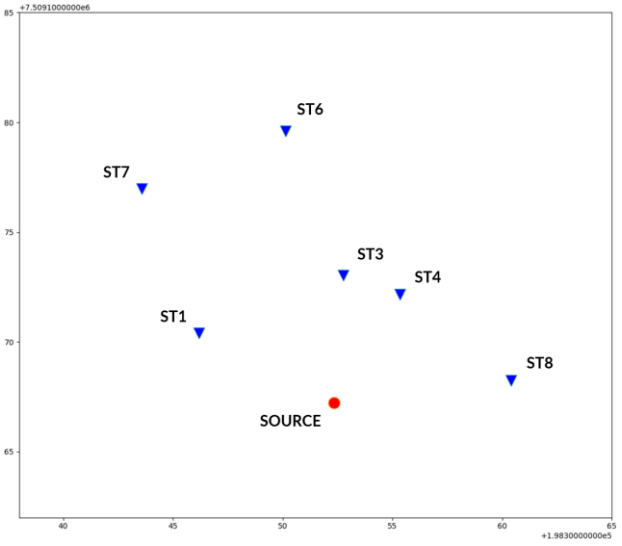

***Figure 10** – Source and stations array map*

Initially, we perform a sensitivity analysis of the event location error according to station geometry. The location error of microseismic events depends on 5 main factors: i) spatial distribution of sensors relative to the source position; ii) inaccuracy of coordinates of the sensors; iii)

errors in determining the arrival time of events (which are associated with system synchronism and the timing of the interpreted wave arrivals); iv) inaccuracy of the velocity model; and v) the location method (which is associated with the mathematical model). Figure 11 shows a location error map for that particular stations and source layout (Figure 10), considering a random error of up to half a millisecond in the wave arrival times.

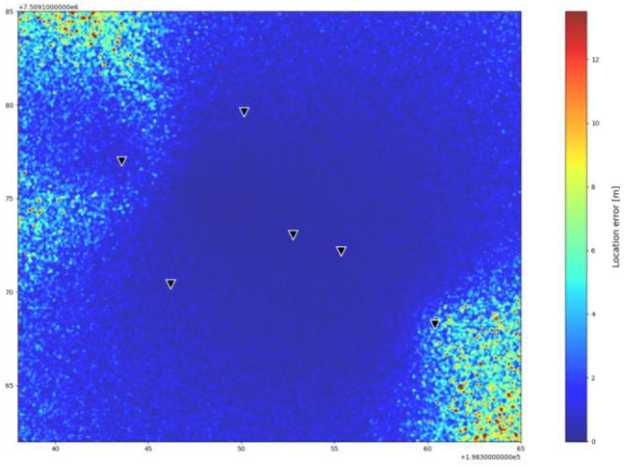

Figure 11 *– Location error sensitivity analysis*

Figure 12 presents the microseismic event record set collected in the experiment, at a sampling rate of 1000 Hz, for each of the 6 stations. This visualization is provided by the backend's processing graphical interface, which allows, for example, the application of filters, zooming, picking of wave arrival times and displaying of amplitude spectra of microseismic records (Figure 13).

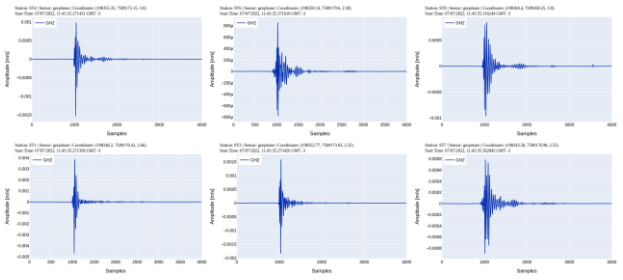

Figure 12 *– Microseismic records collected in the experiment*

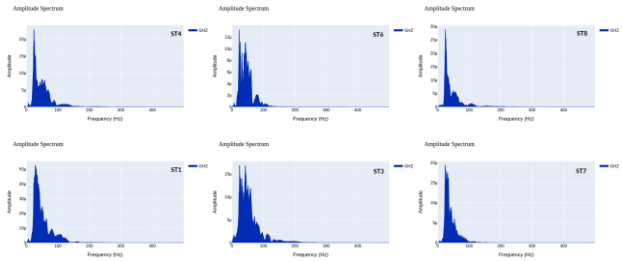

Figure 13 *– Amplitude spectrum of the records*

After processing the event, we obtain the hypocentral distance for each station, the ground motion measurements PGD, PGV and PGA (Table 1) for each microseismic record and also the quantitative properties of the event, such as its geographic location, origin time, local magnitude, corner frequency, seismic potency, seismic moment and moment magnitude (Table 2). The source position and activation time are precisely known for this controlled event. Figure 14 compares the source's estimated (red circle) and true (red dot) positions. Despite all the previously mentioned error sources, the resulting error is only 1 meter, validating the analysis.

Table 1 *– Ground motion measurements*

Station	Hypocenter distance [m]	PGD [μm]	PGV [mm/s]	PGA [m/s²]
ST1	6.21	17.86	4.71	1.34
ST3	4.86	8.51	1.84	0.60
ST4	5.15	6.08	1.54	0.38
ST6	11.52	3.13	0.86	0.25
ST7	12.15	4.36	0.90	0.25
ST8	8.39	4.53	0.97	0.30

Table 2 *– Quantitative properties of the event*

Coordinates (X, Y, Z)	(198352.01, 7509168.23, 0.00)
Origin time	07/07/2022, 11:43:36.269 GMT-3
Local magnitude	-0.7 +- 0.2
Corner frequency [Hz]	54 +- 2
Seismic potency [m³]	0.01
Seismic moment [MN.m]	10.5 +- 5.5
Moment magnitude	-1.4 +- 0.1

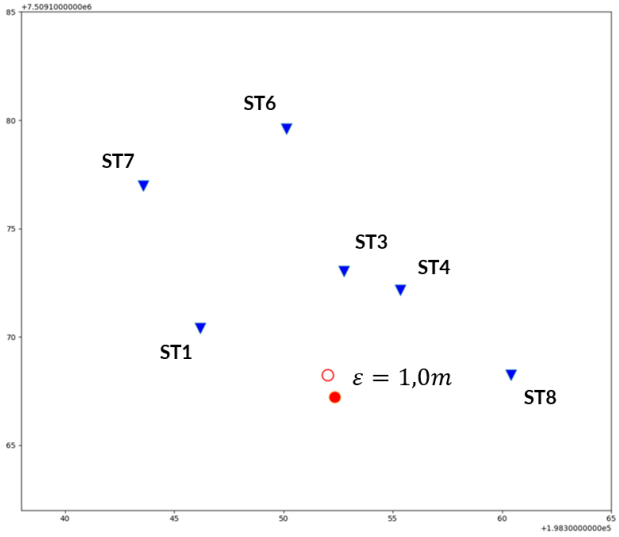

Figure 14 *– Map for comparison between the estimated (red circle) and true (red dot) positions of the source*

Ambient noise passive interferometry

According to Curtis *et al*. (2006), interferometry generally refers to the study of the interference phenomena between pairs of signals to obtain information from their differences. And the main mathematical operation used to study this interference is the cross-correlation between pairs of signals.

From the point of view of Schuster (2016), seismic interferometry is nothing more than the natural displacement of seismic traces so that distant sources or receivers are relocated closer to the interest target.

Planès *et al*. (2016) studied passive seismic interferometry to monitor temporal changes in landfills caused by internal erosion. Failure experiments were monitored at laboratory and field scales. Impulsive responses were reconstructed from ambient noise and temporal variations in seismic wave velocities observed throughout each test.

Olivier *et al*. (2017) demonstrated that this method can be used to monitor the stability of tailings dams over time. Their results indicate that the ambient seismic noise registered by the geophones is suitable for constructing regular and robust virtual seismic sources. In addition, the relative velocity variations achieved were sensitive enough to measure and localize increases in soil fluid saturation due to rainfall. The method also indicated some permanent subsurface changes in the dam wall, in locations consistent with observations of increased seepage.

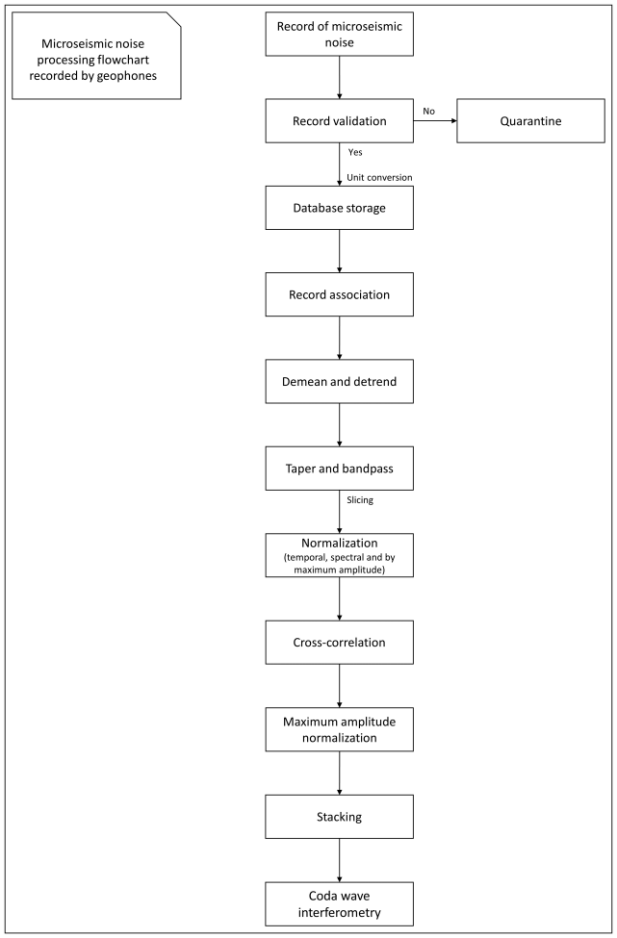

Figure 15 *– Microseismic noise processing workflow*

Figure 15 presents the developed processing workflow of continuous data recorded 24/7, through ambient noise seismic interferometry. Initially, we collect microseismic records with the same start and end time and the same sampling rate for all stations, then the records are validated and stored in the database. After the association, we apply pre-processing tools to remove the instrumental response and frequency band filtering. Next, each record is segmented into smaller windows, and we apply temporal and spectral normalizations to remove the events, keeping only the ambient noise. Then, using the normalized data, we cross-correlate all possible combinations of station pairs, normalizing and stacking the results for each station pair to increase the signal-to-noise ratio. Finally, this stacked cross-correlation function (Green's function of the medium) for the monitor time is compared with the same function of a reference base time through the coda wave interferometry technique. Thus, we estimate the velocity variation in the medium for the period under analysis.

Aiming to validate our processing workflow, we tested it on the data acquired by two stations for 60 days. The uniaxial geophones were installed on the dam crest with a distance of 4 meters between them to monitor the velocity variations in the dam. Initially, the preprocessing step was applied over all database records, including demean, detrend, taper and bandpass filtering (0.1 to 8 Hz). After preprocessing, the records were splitted into 30-minute slices to compute the auto and cross-correlations for the station pairs. During this step, the records were normalized to remove undesirable signals (events) and whitened in the frequency domain. Figure 16 shows the computed cross-correlations between the two sensors data for the 1-day window stack. As observed, we could recover the causal and acausal part of the Green's function of the medium. The red rectangles represent the coda window selected to compute de relative velocity changes in the medium. The reference cross-correlation (baseline) was created considering the first five days of the dataset.

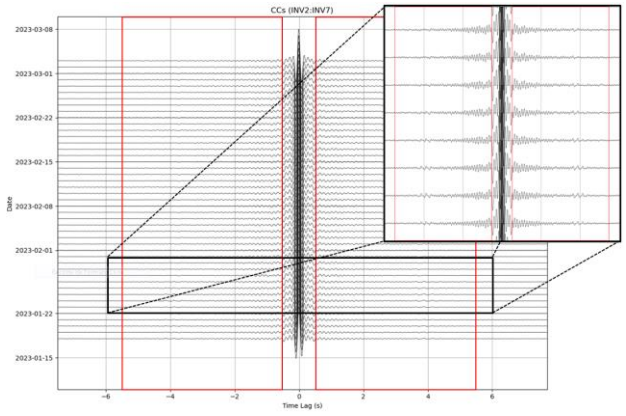

Figure 16 *– The computed cross-correlations between the two sensor data for the 1-day window stack. The red rectangles represent the coda parts (0.5-5.5 seconds) selected to compute the relative velocity changes in the medium*

We estimate the relative velocity variation in the medium for the period under analysis using the Moving Window Cross Spectrum Analysis – MWCS (Clarke *et al*., 2011). The MWCS was computed for 5-day moving window stacks considering both causal and acausal coda parts, with time lags ranging from 0.5 to 5.5 seconds (red rectangles in Figure 16). Figure 17-a shows the

preliminary results of the relative velocity variation in the dam. The curve represents the mean values obtained from the station pair analysis (two auto and one cross-correlation). The green and red arrows indicate the dates of two dam filling-infiltration experiment, where approximately 10 m³ of water was used (total dam capacity). Figure 17-b shows the rainfall data recorded by the Bird Park station (Irioda5, 2023), located approximately 600 meters from the dam. As can be seen, the velocity variation curve presents a good correlation with the pluviometry data. For the base time (01/18–01/22) the dam was already in a state of high-water saturation due to the high precipitation volumes recorded in the previous days. Therefore, the medium's velocity continued to decrease with the rains that occurred on 01/23 and 01/24. After these days, with the decrease in rainfall, the velocity curve increased again, indicating a reduction in water saturation in the soil. The curve only started to decrease again on 02/09, when there were simultaneous rains and the first dam filling-infiltration experiment (green arrow). These events led to a higher variation in the medium's velocity. Then, with the decrease in rainfall, the curve increased again until it stabilized, indicating an increase in the rigidity of the medium. The second dam filling-infiltration experiment produced a smaller velocity variation, possibly related to the lack of rain during that period to reinforce the anomaly like in the previous experiment.

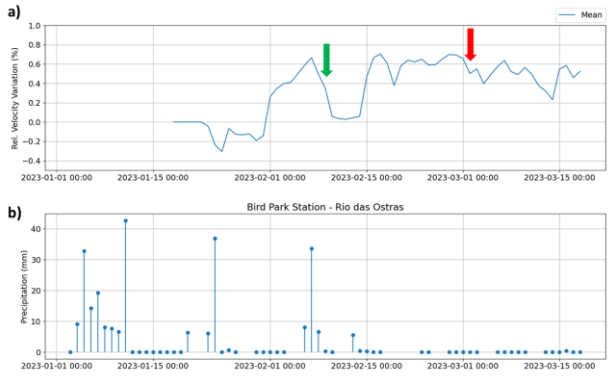

Figure 17 *– (a) Relative seismic velocity variations in the dam. The curve represents the mean values obtained from the station pair analysis (two auto and one cross-correlation). The green and red arrows indicate the dates of the 1st and 2nd reduced-scale reservoir filling-infiltration experiments (b) Precipitation time series registered by Bird Park station, localized approximately 600 meters from the dam*

Conclusions

Our study confirms that microseismic provides quality data to monitor variations in material properties that can be used to assess the safety and stability of tailings dams and other geotechnical structures. The newly developed microseismic monitoring system comprise a set of innovative methodologies, hardware and software. The sensors are designed and built to meet the specifications required to register microseismic events and to operate under adverse environmental conditions. These include high sensitivity, the supply of solar energy and operation via mesh network with wireless communication to facilitate the installation and maintenance of the system in difficult access areas. The field laboratory (reduced-scale dam) was ideal for test-driven system improvements, providing easy access and agile test setups and execution. Furthermore, the experiments demonstrated reliable results in control of the system's health, the high quality of the acquired microseismic data and its processing for events characterization (active sources) and ambient noise seismic interferometry (passive sources).

Acknowledgments

Invision Geophysics would like to thank all multidisciplinary professionals working and who have already worked at some stage in the development of the M²S project, the financial support from FINEP and BNDES, the support from EMBRAPII, the support from Alan Cunha and Marco Braga (CPGA) and SBGf for organizing this congress. We also thank Prof. M. G. A. Justi da Silva for indicating weather stations close to our test site.

References

AZAM, S.; LI, Q. 2010. Tailings dam failures: a review of the last one hundred years. Waste GeoTechnics, Geotechnical News, vol. 28, no. 4, pp. 50–54.

BRAGA, I.L.S.; OLIVEIRA, I.B.; OUVERNEY, G.F.; ASSIS, P.C.; OLIVEIRA, S.A.M.; MORAES, F.S.; PEREIRA, L.D.O.; BRAGA, L.F.S. 2021. Development of a microseismic monitoring system for tailings dams: methodologies, software and sensors. *In*: 17th International Congress of the Brazilian Geophysical Society, Rio de Janeiro, RJ, Brazil.

CLARKE, D.; ZACCARELLI, L.; SHAPIRO, N.M.; BRENGUIER, F. 2011. Assessment of resolution and accuracy of the Moving Window Cross Spectral technique for monitoring crustal temporal variations using ambient seismic noise. Geophysical Journal International, vol. 186, pp. 867–882.

CURTIS, A.; GERSTOFT, P.; SATO, H.; SNIEDER, R.; WAPENAAR, K. 2006. Seismic interferometry – turning noise into signal. The Leading Edge, vol. 25, pp. 1082–1092.

OLIVIER, G.; BRENGUIER, F.; de WIT, T.; LYNCH, R. 2017. Monitoring the stability of tailings dam walls with ambient seismic noise. The Leading Edge, vol. 36, no. 4, pp. 350a1–350a6.

PLANÈS, T.; MOONEY, M.A.; RITTGERS, J.B.R.; PAREKH, M.L.; BEHM, M.; SNIEDER, R. 2016. Time-lapse monitoring of internal erosion in earthen dams and levees using ambient seismic noise. Géotechnique, vol. 66, pp. 301–312.

SCHUSTER, G.T. 2016. Seismic interferometry. *In*: Encyclopedia of Exploration Geophysics, Society of Exploration Geophysicists, Tulsa, OK, USA, pp. Q1-1–Q1-41.

IRIODA5, "Estação Parque dos Pássaros, Rio das Ostras, RJ, Brasil", accessed May 18, 2023, https://www.wunderground.com/dashboard/pws/IRIODA5.